PROPAGATION OF A TURBULENT JET IMPACTING ON A FLAT SURFACE

O. V. Yakolevskiy, S. Yu. Krashennikov

NASA TT F-10,784

Translation of "Rasprostranenye turbulentnoy struy, soudaryayushcheysya s ploskoy poverkhnost'yu". Izvestiya Akademii Nauk SSSR, Mekhanika Zhidkosti i Gaza, No. 4, pp. 192-197, 1966.

NATIONAL AERONAUTICS AND SPACE ADMINISTRATION
WASHINGTON D.C. MARCH 1967

PROPAGATION OF A TURBULENT JET IMPACTING ON A FLAT SURFACE

O. V. Yakolevskiy, S. Yu. Krashennikov
(Moscow)

Consideration of the flow phenomena caused by the collision of a turbulent jet with a flat surface at a certain angle of incidence. Such problems originate in static tests, in the study of the "ground effect" manifested in the appearance of velocity and temperature discontinuities at engine intake for aircraft with vertical or short takeoff, or in ventilation equipment, etc. Test results are used as the basis for derivation of formulas for approximate calculation of the flow phenomena.

This article gives the results of studying flows caused by the impact of a /192* turbulent jet on a flat screen at a certain angle. Problems of this sort occur, for example, in stand tests when studying the "Earth proximity" effect (Ref. 1) which manifests itself in the appearance of velocity and temperature irregularities at the input of motors in devices with vertical or shortened takeoff and landing characteristics, in ventilation engineering, etc. (Ref. 2, 3).

1. Experiments were conducted on an installation which made it possible to study the propagation of an air jet across a disk 400 mm in diameter. The jet impacted on the disk at angles of 30, 45, 60 and 90°, while distance l from nozzle edge to the disk along the jet axis was 35 and 100 mm with a nozzle radius of R_0 = 5 mm. The investigated flow is therefore the flow of a jet colliding with a screen both in its initial sector ($l^\circ = l/R_0 = 7$) and in its main portion ($l^\circ = 20$). The system of coordinate points permitted determination of the field of velocity heads in arbitrary directions on the disk surface and travel of these fields along the vertical (the disk was placed horizontally). Accuracy of displacement of the Pitot-static head was 0.5 mm. Air flow rate was recorded with an accuracy of 2-3% by a standard measuring diaphragm. Air velocity at nozzle outlet in the experiments was 103 m/sec and did not vary. The velocity head fields were determined with an accuracy of 0.2 mm H_2O from the readings of an alcohol micromanometer. The disk was bled radially every 5 mm. The bleed holes were used to measure static pressure. The velocity head fields were recorded on radii forming angles ψ = 0, 45, 90, 135 and 180° with the projection of the jet axis onto the disk. These radii were drawn from the point of intersection 0_ψ of the jet axis with the disk plane.

Figure 1 gives the results of measuring velocity distribution along the vertical at different points on the disk. It may be seen that the profiles of relative velocity as a function of the coordinates u° and z° are similar. We used maximum velocity at given disk point u_m and jet half-thickness $z_{0.5}$ as the characteristic scales of velocity and length in the expressions $u^\circ \equiv u/u_m$

* Numbers in the margin indicate pagination in the original foreign text.

and $z^\circ \equiv z/z_{0.5}$, which corresponds to the vertical distance from the disk to the point at which $u = 0.5\ u_m$.

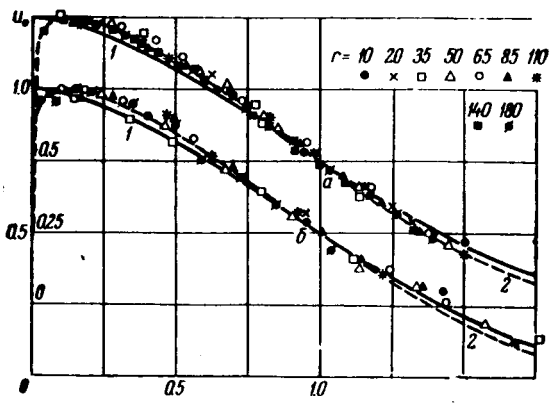

Figure 1

Relative Velocity Distribution u° Over Jet Thickness. a - $\theta = 90°$, $l^\circ = 7$; b - $\theta = 45°$, $l^\circ = 7$, $\psi = 0°$.

1 -- Schlichting profile; 2 -- The same taking the boundary layer into account.

Figure 1 demonstrates the fact that the velocity profile is well-described by Schlichting's formula

$$u^\circ = (1 - \xi^{3/2})^2 \text{ when } z \geqslant \delta, \qquad \xi = \frac{z - \delta}{b - \delta}$$
$$u^\circ = (z/\delta)^{1/n} \text{ when } z \leqslant \delta$$

Here δ is the thickness of the boundary layer; b is jet thickness [n was not established in the experiments, but from data in (Ref. 4) for semi-limited jets $n \approx 10$).

Figure 2 represents the dependences of $z_{0.5}$ on radius r -- the distance from point 0_ψ -- for various impact angles θ. From the Schlichting velocity profile (allowing for the boundary layer) we may derive the dependence -16(-)-16 of jet thickness on r

$$\frac{b - b_*(\psi)}{r - r_*(\psi)} = c \approx 0.16 \qquad (1.1)$$

where $b_*(\psi)$ and $r_*(\psi)$ are certain initial values of jet thickness and radius. We utilized the fact that in the above-given velocity profile the relationship $z_{0.5} = (0.44 - 0.5)$ holds, depending on boundary layer thickness. Measurements indicated that boundary layer thickness (distance from disk surface to point of maximum velocity) was 5 - 10% of jet thickness in the experiments conducted.

From the measurement results we plotted the distribution of maximum velocities in the disk plane (Figure 3). As we can see, the isotach shape as point 0_ψ is approached does not differ greatly from a circular shape. Figure 4 presents findings characterizing the attenuation of maximum velocity u°_m as one recedes from the impact region.

2. The experimental data obtained underlie the flow diagram, which made it possible to give an approximate calculation of the flow. Figure 5 gives the schematic picture of jet propagation which was used as the basis of the calculations. Let us present the features of the flow model adopted in the computations. The basic assumption, which is to a certain degree confirmed by the data in Figure 3, is that after the jet is deflected, the flow has a form which would occur on efflux from a circular cylindrical source of variable height b_*. The center of this source 0_ϕ is displaced by an amount Δ (see Figure 5) relative to the point 0_ψ of intersection of the jet and the screen

/193

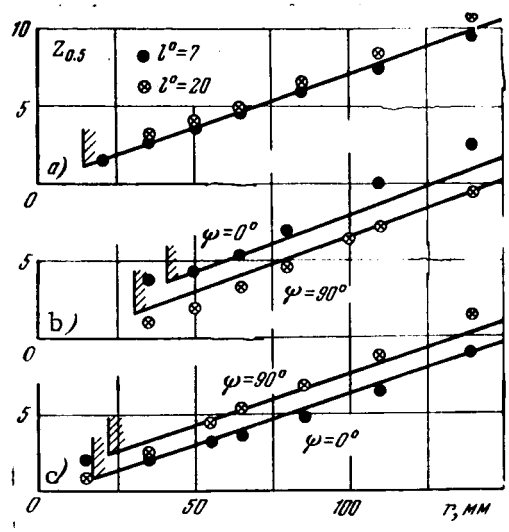

Figure 2

Change in Jet Half-thickness $z_{0.5}$ as One Recedes from the Deflection Zone:
a - $\theta = 90°$; b - $\theta = 60°$, $l° = 20$; c - $\theta = 45°$, $l° = 7$.
Verticle line with hatching corresponds to $r = r_*$.

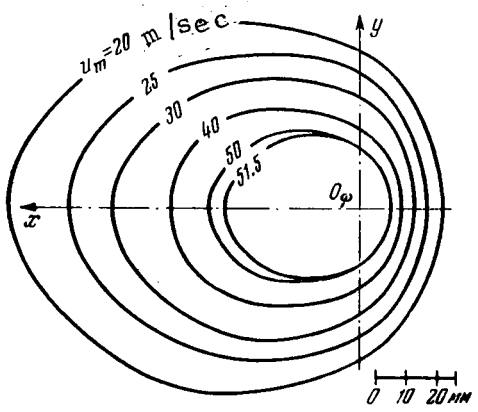

Figure 3

Lines of Equal Maximum Velocity Values (Isotachs or Isovels) when $\theta = 45°$ and $l° = 20°$.

plane. Velocity at source outlet is constant and equals u_{m*}. Efflux takes place in the direction of the radii drawn from O_ψ (this is confirmed by measurements).

Measurements of the static pressure showed that in the vicinity of the deflection zone (outside the source) this pressure differs from atmospheric pressure by no more than 2 - 3% of the maximum velocity head at the corresponding disk point. When one recedes farther from O_ψ, it tends toward atmospheric pressure. This circumstance fosters the assumption that the jet is isobaric in its propagation over the screen.

In conformity with the experimental findings, it may be hypothesized that the upper base of the cylindrical source is a plane forming a certain angle with the plane of the screen. In this case, the height of the annular source generatrixes, depending on the direction of propagation, will be expressed by the relationship

$$b_* = A + B\cos\varphi \qquad (2.1)$$

Angle ϕ differs from ψ by an amount ε dependent on ψ (see Figure 5).

To determine the flow at the source outlet, the three geometric parameters A, B, and Δ must be found, which depend on the angle θ between the impact direction of the jet and the screen plane and on longitudinal velocity profile shape in the free jet before the deflection zone . We must also find a kinematic parameter u_{m*} which depends on magnitude and distribution of the velocity w at

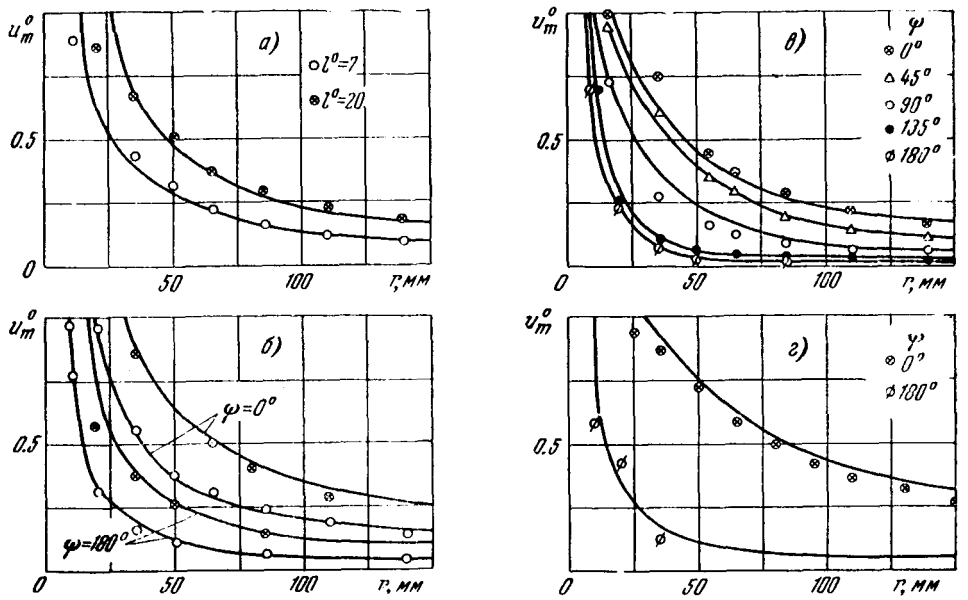

Figure 4

Damping of Maximum Velocity u°_m as One Recedes from the Deflection Zone. a - $\theta = 90°$; b - $\theta = 60°$, $l° = 20$, $l° = 7$; c - $\theta = 45°$, $l° = 7$; d - $\theta = 30°$, $l° = 20$.

the inlet to the annular source. The jet parameters immediately in front of the deflection zone, which may be approximately identified with the annular source, are determined by the known laws for a turbulent jet (Ref. 5). The justification for this is that the presence of the screen exerts no essential effect on the flow in the jet right up to the deflection zone (Ref. 1).

3. To determine the magnitude of maximum velocity at the annular source outlet, let us assume that total flux and kinetic flow energy, i.e.,

$$\int_{t_*}\int_{0}^{b_*} u\cos\varepsilon\, dz\, dt = \int_{s_*} wr\, ds$$
$$\int_{t_*}\int_{0}^{b_*} u^3\cos\varepsilon\, dz\, dt = \int_{s_*} w^3 r\, ds \qquad (3.1)$$

are maintained in the deflection process.

Here ε is the angle between vector radii r and ρ drawn in the screen plane from points 0_ψ and 0_ϕ, respectively (Figure 5); t_* is the boundary of the annular source base; b_* is the height of the cylinder generatrix; z is the coordinate axis normal to the screen plane; s_0 is the area of the free jet cross section at the inlet to the deflection zone. Assuming that the velocity profiles do not depend on ϕ, i.e., /194

$$u_*(z^\circ) = u_{m^*} f(z^\circ), \quad z^\circ = z/b_*, \quad w_*(R^\circ) = w_{m^*} f_0(R^\circ), \quad R^\circ = R/R_* \tag{3.2}$$

we may transform relationship (3.1) to the form

$$\int_0^1 f(z^\circ)\,dz^\circ \int_{t_*} b_* u_{m_*} \cos\varepsilon\,dt = \pi R_*^2 \int_0^1 f_0(R^\circ)\,R^\circ w_{m^*}\,dR^\circ$$
$$\int_0^1 f^3(z^\circ)\,dz^\circ \int_{t_*} b_* u_{m^*}^3 \cos\varepsilon\,dt = \pi R_*^2 \int_0^1 f_0^3(R^\circ)\,R^\circ w_{m^*}^3\,dR^\circ \tag{3.3}$$

Here R is the radial distance between free jet axis and an arbitrary point; R_* is the boundary radius of the free jet before the deflection zone; w_{m*} is the maximum velocity (on the axis) in the jet before the deflection zone; and u_{m*} is maximum velocity at annular source outlet (does not depend on ϕ). Solving system (3.3), we obtain

$$u_{m^*} = \alpha w_{m^*} \tag{3.4}$$

$$\alpha = \left(\int_0^1 f_0^3(R^\circ)\,R^\circ\,dR^\circ \int_0^1 f(z^\circ)\,dz^\circ\right)^{1/2} \left(\int_0^1 f_0(R^\circ)\,R^\circ\,dR^\circ \int_0^1 f^3(z^\circ)\,dz^\circ\right)^{-1/2} \tag{3.5}$$

(in the case of Schlichting profile, $\alpha = 0.778$).

To find parameters A and B in expression (2.1), we employ the conditions for the maintenance of flow rate and of momentum projected onto the screen plane. Employing expressions (2.1), (3.2), and (3.5) we may write these conditions as

$$2\rho \int_0^\pi (A + B\cos\varphi)\cos\varepsilon\,d\varphi = \frac{s_0}{\alpha}\beta, \quad 2\rho \int_0^\pi (A + B\cos\varphi)\cos\varepsilon\cos\psi\,d\varphi = \frac{s_0}{\alpha^2}\gamma\lambda \tag{3.6}$$

Here, in addition to annular source radius ρ, the following notation is introduced: $\lambda = \cos\theta$.

$$\beta = 2\left(\int_0^1 f_0(R^\circ)\,R^\circ\,dR^\circ\right)\left(\int_0^1 f(z^\circ)\,dz^\circ\right)^{-1}, \qquad \gamma = 2\left(\int_0^1 f_0^2(R^\circ)\,R^\circ\,dR^\circ\right)\left(\int_0^1 f^2(z^\circ)\,dz^\circ\right)^{-1}$$

In view of the geometric deflection diagram, we may write the expression /195

$$\cos\varepsilon = \frac{\mathbf{r}\boldsymbol{\rho}}{|\mathbf{r}|\cdot|\boldsymbol{\rho}|}, \quad \text{or} \quad \cos\varepsilon = \frac{\rho + \Delta\cos\varphi}{\sqrt{\rho^2 + 2\rho\Delta\cos\varphi + \Delta^2}} \tag{3.7}$$

By using the relationships derived and neglecting the change in cos ε with respect to the change in cos ψ, we may derive the flow rate and momentum equation in the form

$$A(I_0 + \Delta^\circ I_1) + B(I_1 + \Delta^\circ I_2) = \frac{s_0}{2\rho\alpha}\beta, \quad A(I_1 + \Delta^\circ I_0) + B(I_2 + \Delta^\circ I_1) = \frac{s_0\gamma\lambda}{2\rho\alpha^2} \tag{3.8}$$

Here the following notation is used:

$$\Delta^\circ = \frac{\Delta}{\rho}; \qquad I_i = \int_0^\pi \frac{\cos^i\varphi\,d\varphi}{\sqrt{1 + 2\Delta^\circ\cos\varphi + \Delta^{\circ 2}}} \qquad (i = 0, 1, 2).$$

The calculations demonstrate that

$$A = \frac{s_0\beta}{2\rho\alpha(I_0 + \Delta^\circ I_1)} \quad (0 \leqslant \Delta^\circ \leqslant 0.85), \quad A = \frac{s_0\beta}{2\rho\alpha\pi} \quad (\Delta^\circ < 0.6) \tag{3.9}$$

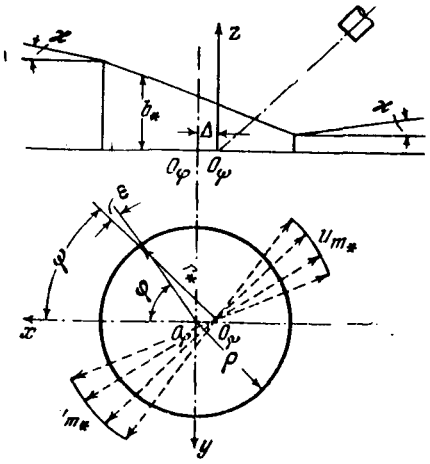

Figure 5

Diagram of Jet Propagation.

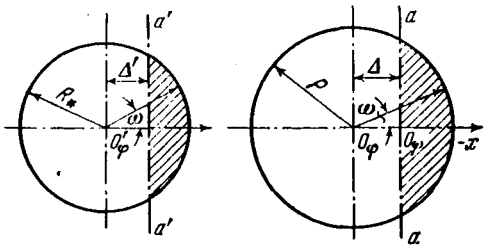

Figure 6

Illustrating How Flow Rate Balance is Determined.

This result means that average deflection zone height is practically independent of the angle at which the jet strikes the screen.

In order to find the fourth unknown Δ°, the system of these conservation equations must still be closed by a single relationship. When the deflection of ideal liquid jets is calculated (Ref. 6), the assumption is made that flow in the angle element before and behind the deflection zone is maintained. A similar assumption, but in integral form, may be made in the case under consideration. Figure 6 shows the cross section of the jet before the deflection zone, and the base of the cylinder is the annular source. By drawing the straight line a-a perpendicular to the x-axis through O_ψ in the plane of the cylinder base, we delimit the liquid flow into two parts: All the liquid to the right of a-a will move to the right, while all the liquid to the left of this line will go to the left. In the transverse jet cross section s_0 at a certain distance Δ' from the jet axis, a straight line a'-a' perpendicular to the x-axis may also be drawn: The liquid to the left of a'-a' will move to the left after the turn, and the liquid to the right of a'-a', to the right. Let us assume by analogy with the ideal liquid theory that distances Δ and Δ' are proportional to the radii of the corresponding circles

$$\frac{\Delta'}{R_*} = \frac{\Delta}{\rho} = \Delta^\circ \tag{3.10}$$

This relationship closes the system.

Based on the adopted flow diagram,we may state the flow rate balance. With allowance for the second relationship in expressions (3.9) and (3.10), as well as disregarding the change in cos ε, the condition for flow rate equality through the unshaded part of the cross secitn in Figure 6 gives

$$B\sqrt{1-\Delta^{\circ 2}} = \frac{R_*^2 w_{m*}}{\rho u_{m*}} \left(\int_0^1 f(z^\circ)\,dz^\circ\right)^{-1} \int_0^{\arccos \Delta^\circ} \int_0^{\Delta^\circ/\cos\omega} f_0(R^\circ)\, R^\circ\, dR^\circ d\omega \tag{3.11}$$

Angle ω is measured from the negative x-axis direction, i.e., $\omega = \pi - \phi$. /196

Joint solution of equations (3.8) and (3.11) makes it possible to find the quantities B and Δ° depending on λ and the velocity profile shape in the jet before the deflection zone.

The calculations showed that the relationship

$$\Delta^\circ = \frac{\Delta}{\rho} = \lambda \left(2\int_0^1 f_0(R^\circ)\, R^\circ dR^\circ\right)^{1/2} \tag{3.12}$$

is fulfilled in a wide range of λ values.

For an ideal liquid jet (rectangular velocity profile) equation (3.12) changes into the relationship $\Delta^\circ = \lambda$ derived by Schach (Ref. 6).

Utilizing the above-derived results, let us write out the final formulas for calculating the annular source parameters:

$$u_{m_*} = \alpha w_{m_*}, \quad A^\circ = \frac{\beta\pi}{2\alpha(I_0 + \Delta^\circ I_1)}, \quad \left(A^\circ \approx \frac{\beta}{2\alpha} \text{ for } \Delta^\circ < 0{,}6\right)$$
$$B^\circ = \frac{-A^\circ[\Delta^\circ I_0 + I_1] + \frac{1}{2}\pi\gamma\lambda\alpha^{-2}}{I_2 + \Delta^\circ I_1}, \quad \Delta^\circ = \lambda\left(2\int_0^1 f_0(R^\circ)\, R^\circ dR^\circ\right)^{1/2} \tag{3.13}$$
$$A^\circ = k\,A/R_*, \qquad B^\circ = k\,B/R_*, \qquad k = \rho/R_*$$

The approximation formula (3.12) for Δ° may be employed in the value range $0 \leq \lambda \leq 0.7$, which corresponds to impact angles $90^\circ \geq \theta \geq 45^\circ$. For large values of λ, Δ° may be obtained either by numerical integration or by extrapolation using the condition $\lambda = 1$, $\Delta^\circ = 1$.

The quantity k introduced above is an experimental constant. It was found from the condition of best agreement between quantities b_* and r_* in relationship (1.1) when drawing lines corresponding to $z_{0.5}$ in Figure 2, and proved to equal 1.5. The quantities b_* and r_* are connected by relationships (3.13), since condition (2.1) holds.

4. To describe the further propagation of the jet over the plane, we may use the experimental relationship (1.1). Let us examine the motion of the liquid element in cylindrical coordinates, while the z axis is perpendicular to the screen plane and the coordinate origin is at point 0_ψ. We will write the law of change in momentum for the liquid volume element with the length dr; this volume is delimited by two planes which make the angle $d\psi$ and passing through the z axis,

$$\int_0^{b_1} u_1^2 dz_1 dL_1 = \int_0^{b_2} u_2^2 dz_2 dL_2 + T dF_1 - (Q - Q')\, dF_2 \tag{4.1}$$

Here b is the element height; L is the arc delimiting the element; T is friction stress on the lower face of element F_1; and Q, Q' is the direction of turbulent friction on the side faces F_2. (The action of pressure forces is mutually balanced out.) Letting the longitudinal and transverse dimensions of the element tend toward zero, as well as employing formula (1.1), the geometric

relationships

$$b_1 = (r - r_*)c + b_*, \quad b_2 = (r + dr - r_*)\,c + b_*, \quad dL_1 = rd\psi, \quad dL_2 = (r + dr)\,d\psi$$

and the conditions of similitude of velocity profiles, we may derive the following differential equation

$$r\,[(r - r_*)\,c + b_*]\frac{du_m^2}{dr} - u_m^2\,[(2r - r_*)\,c + b_*] - \frac{T}{J} + \frac{b}{J}\frac{dQ}{d\psi} = 0 \quad \left(J = \int_0^1 f^2(z^\circ)\,dz^\circ\right) \qquad (4.2)$$

after omitting the terms of the second order of smallness.

Calculations have shown that the third term of equation (4.2) when the Reynolds number is $R = 7 \cdot 10^4$ (computed from the nozzle diameter and efflux parameters), which occurred in the experiments, is no more than 4.5% of the value of the left side. At large Reynolds number values, which are to be expected in cases of practical interest, this term is still smaller. The maximum value of the fourth term does not exceed 2.5% of the sum of the terms on the left side. After these terms have been disregarded, equation (4.2) may be integrated by using the following condition

$$r = r_*, \qquad u_m = u_{m^*} = \alpha w_{m^*}$$

Thus we obtain

$$u_m^2 = \alpha^2 w_{m*}^2 \cdot \frac{r_*}{r}\left[1 + \frac{ck^2}{A^\circ + B^\circ \cos\varphi}\left(\frac{r}{r_*} - 1\right)\right]^{-1}$$
$$r_* = \rho\,(\sqrt{1 + \Delta^{\circ 2}\sin^2\psi} + \Delta^\circ \cos\psi), \quad \cos\varphi = -\Delta^\circ \sin^2\psi + \cos\psi\,\sqrt{1 + \Delta^{\circ 2}\sin^2\psi} \qquad (4.3)$$

Parameters A°, B°, Δ°, and α are found from formulas (3.13), (3.12), and (3.5). The angle determining the propagation direction is ψ; angle ϕ plays an auxiliary role and serves to describe the geometrical picture of the deflection. /197

If, before impact with the screen, the maximum velocity on the jet axis in the free jet is $w_m \sim 1/l$ and the jet radius is $R \sim l$, which corresponds to the experimental findings, then from the relationships (4.3) it follows that for sufficiently large values of r, the value of maximum velocity u_m at an arbitrary point in the screen does not depend on l and is determined only by angle θ. This fact is corroborated by the experiments conducted in the present work.

The case of forward collision of the jet against the plane ($\theta = 90°$) explained in (Ref. 1) is derived for $B^\circ = 0$. In this case the first relationship (4.3) is converted into the corresponding relationship obtained in (Ref. 1).

5. In order to employ the formulas for computing flow over the screen, we must know the jet parameters in front of the deflection zone. These parameters are determined from the familiar formulas quoted, for example, in (Ref. 1):

$$w_{m^*}/w_{m_0} = 1, \quad R_*/R_0 = k_2' l^\circ + 1 \text{ when } l^\circ \leqslant 12$$
$$w_{m^*}/w_{m_0} = k_3/l^\circ, \quad R_*/R_0 = k_2 l^\circ \text{ when } l^\circ \geqslant 12$$
$$k_2 = 0.22, \quad k_2' = 0.14, \quad k_3 = 12.4.$$

Determination of the velocity profiles at entry into the deflection zone when $\bar{l} < 12$ requires a knowledge of ordinate R_1 of the internal boundary of the displacement zone, as determined from the formula $(R_0 - R_1)/R_0 = 0.13\,\bar{l}^\circ$.

The relationship

$$\int_0^1 f_0^n(R^\circ)\,R^\circ\,dR^\circ = 0{,}5\,(R_1^\circ)^2 + (1 - R_1^\circ)^2 \int_0^1 f_{00}^n(\eta)\,\eta\,d\eta + (1 - R_1^\circ)\,R_1^\circ \int_0^1 f_{00}^n(\eta)\,d\eta$$

$$R_1^\circ = \frac{R_1}{R_*}; \qquad \eta = \frac{R - R_1}{R_* - R_1}$$

may be utilized to compute the quantities α, β and γ in the initial sector of the jet.

In the computations carried out in the present paper, Schlichting's formula

$$f_{00}(\eta) = (1 - \eta^{3/2})^2$$

was used to describe the velocity profile in front of the deflection zone.

To describe the velocity profile at the outlet of the annular source and during further propagation of the jet over the screen, we used Schlichting's profile taking into consideration the boundary layer (see Figure 1)

$$u^\circ = (z/\delta)^{1/n} \text{ for } z \leqslant \delta; \quad u^\circ = [1 - (z - \delta)^{3/2}(b - \delta)^{-3/2}]^2 \text{ for } \delta \leqslant z \leqslant b$$

The position of the upper base of the annular source is not known in advance; therefore, the parameters of the jet before the impact zone are computed by successive approximations. First the geometric parameters of the deflection zone and of the annular source are computed in terms of distance from nozzle to screen $\bar{l}$; then the correction is introduced for the finite thickness of the deflection zone. Two approximations are usually quire adequate.

Figure 4 gives the computational results together with the experimental findings on damping of maximum velocity $u^\circ_m = u_m/w_{m*}$. A comparison discloses their satisfactory correspondence.

In conclusion, the authors would like to thank G. B. Krayushkina, who participated in conducting the experiments and formulating the results of the work.

Received November 30, 1965

REFERENCES

1. Yakovlevskiy, O. V., Sekundov, A. N. "Investigation of the Interaction of a Jet with Closely Placed Screens", Izvestiya Akademii Nauk SSSR, Mechanika i Mashinostroyeniye, No. 1, 1964.
2. Shamtsiyan, G. G. "Tolerable Temperature of a Cold Air Jet Delivered to a Room", Vodosnabzheniye i Sanitarnaya Tekhnika, No. 9, 1963.
3. Sychev, A. T. "Research Results on a Submerged Turbulent Jet Flowing into the Plane of a Smooth Ceiling", Izhenerno-Fizicheskiy Zhurnal, Vol. 7,

No. 3, 1964.
4. Sakinov, Z. B. "Experimental Investigation of Semi-Restricted Jets", Problemy Teploenergetiki i Prikladnoy Teplofiziki. Vyp. I. Prikladnaya teplofizika. Izdatel'stvo Akademii Nauk KazSSR, Alma-Ata, 1964.
5. Abramovich, G. N. Teoriya turbulentnykh struy (Theory of Turbulent Jets). Fizmatgiz, Moscow, 1960.
6. Schach, W. "Deflection of Free Liquid Jet on a Smooth Plate", Ingenieur-Archiv, Vol. 5, No. 4, 1934.

Scientific Translation Service
4849 Tocaloma Lane
La Canada, California